



Room temperature volatile organic compounds sensor with enhanced performance, fast response and recovery based on N-doped graphene quantum dots and poly(3,4-ethylenedioxythiophene)-poly(styrenesulfonate) nanocomposite

Journal:	<i>RSC Advances</i>
Manuscript ID:	RA-ART-05-2015-008158.R1
Article Type:	Paper
Date Submitted by the Author:	15-Jun-2015
Complete List of Authors:	nasrollah gavgani, jaber; Amirkabir University of Technology, Polymer Engineering and Colour Technology Sharifi Dehsari, Hamed; Amirkabir University of Technology (Tehran Polytechnic), Polymer Engineering and Color Technology Department Hasani, Amirhossein; K.N. Toosi university of technology, electrical engineering Mahyari, Mojtaba; Department of Chemistry, Shahid Beheshti University, Khodabakhshi shalamzari, Elham; Amirkabir University of Technology (Tehran Polytechnic), Polymer Engineering and Color Technology Department Salehi, Alireza; K.N. Toosi University of Technology, Department of Electrical Engineering Afshar Taromi, Faramarz; Amirkabir University of Technology (Tehran Polytechnic), Polymer Engineering and Color Technology Department

Room temperature volatile organic compounds sensor with enhanced performance, fast response and recovery based on N-doped graphene quantum dots and poly(3,4-ethylenedioxythiophene)-poly(styrenesulfonate) nanocomposite

Jaber Nasrollah Gavvani^a, Hamed Sharifi Dehsari^a, Amirhossein Hasani^c, Mojtaba Mahyari^{*b}, Elham Khodabakhshi Shalamzari^a, Alireza Salehi^c, Farmarz Afshar Taromi^{*a}

- a) Department of Polymer Engineering and Color Technology, Amirkabir University of Technology, P.O.Box 15875-4413, Tehran, Iran
- b) Department of Chemistry, Shahid Beheshti University, G. C., P.O.Box 19396-4716, Tehran, Iran
- c) Department of Electrical Engineering, K.N. Toosi University of Technology, P.O.Box 16315-1355, Tehran, Iran

*Email address: afshar@aut.ac.ir; m_mahyari@sbu.ac.ir
Tel: +982164542401
First two authors contributed equally to this work.

Abstract

The highly efficient, and facile sensing system made of N-doped graphene quantum dots (N-GQDs)/poly(3,4-ethylenedioxythiophene)-poly(styrenesulfonate)(PEDOT-PSS) was fabricated by drop coating on interdigitated Au electrodes with high uniformity over a large area of silicon substrate and was used to sense vapors of volatile organic compounds (VOCs) detection at room temperature. An innovative method was developed for the synthesis of N-GQDs by hydrothermal process of citric acid. The N-GQDs obtained have a N to C atomic ratio of 0.058 and diameter of 2–7 nm. The nanocomposite sensing system exhibits high sensitive, selective, rapid, and reversible responses for detection of 1-1000 ppm VOCs. The N-GQDs/PEDOT-PSS nanocomposite gas sensor enhance methanol sensing properties by 13 times compared to pristine PEDOT-PSS in a low concentration of 50 ppm methanol. Moreover, the gas sensor based on the nanocomposites have fast response (ca. 12 s) and recovery (ca. 32 s) behavior, excellent room temperature selectivity and stability. The methanol-sensing mechanisms of the N-GQDs/PEDOT-PSS nanocomposite gas sensor based on direct charge transfers and swelling process are highlighted.

Keywords: N-doped graphene quantum dots, volatile organic compounds, PEDOT-PSS, sensitivity

Introduction

Volatile organic compounds (VOCs) have been released by agricultural, industrial, and human activities [1-3]. The concentration of VOCs should be strictly controlled, namely neither too low nor too high. Nevertheless, free VOCs with too high of a level may also be harmful, because these could react with oxygen based free radicals to produce new toxic products have been proclaimed to be potentially dangerous to human beings and animals; for example, they may result in cancer, allergies, cardiovascular system, respiratory tract, asthma, and emphysema [4-6]. Therefore, it is essential to monitor the concentration of VOCs in environment. Continuing interest is focused on the development of VOCs sensors with higher sensitivity, broad VOCs detection range, as well as rapid response and recovery times for the determination and control of VOCs in environment. To achieve these goals, considerable attention has been directed toward the development of VOCs sensitive materials, especially nanomaterials due to their high surface to volume ratio and combination of conjugated polymers with nanomaterials [7-11]. However these sensors suffer from their respective disadvantages, such as the requirement for many types of reagents that may produce strong toxicity, low detection sensitivity, poor selectivity, limited structural and chemical properties, long response time and complicated performance [12,10,13]. Therefore, developing a low cost and facial VOCs sensing material that possesses high and even sensitivity for the full range of VOCs remains a challenge.

Graphene quantum dots (GQDs), as recently emerging carbon-based materials, are graphene sheets smaller than 100 nm are proposed to be promising substitutes of the heavy-metal-containing semiconductor-based QDs [14]. The GQDs have attracted more and more attention

due to their special advantages, such as low toxicity, better surface grafting properties because of their π - π conjugated networks or surface groups, high fluorescent activity, robust chemical inertness, and excellent photostability [14-18]. However, to date, nearly all research is focused on their preparation and property study; while little attention has been paid to the applications of the GQDs except for their applications in bioimaging, photoreduction of metals, and optoelectronic devices. To the best of our knowledge, there are no studies of the application of GQDs in VOCs sensing material. Herein, due to our interest in synthesis of graphene based materials for various applications [19-23], especially as sensor [24-26], an effectively facile one step route has been presented to synthesis of N-doped GQDs (N-GQDs) by a hydrothermal process of citric acid. Herein we fabricated a sensitive, selective, facile, and low cost VOCs gas sensor based on pristine N-GQDs, pure Poly (3,4 ethylenedioxythiophene)-poly(styrenesulfonate) (PEDOT-PSS), and N-GQDs/PEDOT-PSS nanocomposite. It is evident from the present work that room-temperature VOCs sensor with enhanced performance, fast response and recovery behavior using N-GQDs/PEDOT-PSS nanocomposite, suggesting promising applications of GQDs in sensing applications.

Experimental section

Materials

The poly (3,4 ethylenedioxythiophene)-poly(styrenesulfonate) aqueous solution (PEDOT-PSS, weight ratio = 1:6, Clevios™ P VP AI 4083, solid content 1.3–1.7 %) was purchased from Heraeus Precious Metals GmbH & Co., KG. Dimethyl sulfoxide (DMSO) was purchased from Merck Co. Citric acid (+99.5 %), Urea (98 %), and ethanol were purchased from Sigma Alderich Co. Doubly distilled (DI) water was used throughout the experiment.

Synthesis of N-doped GQDs (N-GQDs)

N-GQDs were synthesized by hydrothermal process of citric acid and urea. Briefly, citric acid (0.21 g, 1 mmol) and urea (0.18 g, 3 mmol) were dissolved in water (5 mL) and stirred about 30 min, until the solution was made clear. Subsequently, the suspension was transferred into a 100 mL Teflon-lined autoclave and heated to 160 °C for 4 h. Then, 50 mL ethanol was added to suspension drop by drop, with continuous, vigorous stirring. After cooling to room temperature, the resulting black suspension was centrifuged at 6000 rpm for 10 min and N-GQDs were obtained.

Preparation of N-GQDs/PEDOT-PSS nanocomposite

For preparation of the N-GQDs/PEDOT-PSS nanocomposite, PEDOT-PSS was first dissolved in a DI water with a weight concentration of 89.82 %. To prepare N-GQDs solution, 10 mg of hydrothermally synthesized N-GQDs powder was dispersed in 5 mL of DI water. The N-GQDs solution was then thoroughly sonicated with ultrasonication bath (EUROSONIC® 4D, 50 kHz) for 30 min at room temperature. Next, N-GQDs solution and 6 wt% DMSO were added into the PEDOT-PSS solution and a homogeneous aqueous dispersion was obtained after 1 h sonication and stirred for 4 h.

Fabrication of N-GQDs/PEDOT-PSS nanocomposite gas sensor

For fabrication of N-GQDs/PEDOT-PSS nanocomposite gas sensor, interdigitated Au electrodes with 100 nm thickness were deposited on a SiO₂/Si substrate (10×4 mm²) by physical vapor deposition method (Fig. 1a-c). The prepared N-GQDs/PEDOT-PSS nanocomposite solution was

then drop casted over an interdigitated electrode (Fig. 1d). The width and inter-spacing of the electrodes are 200 μm and 400 μm , respectively. Then the nanocomposite gas sensor was backed for 1 h in furnace (Exciton, EX1200-4L) at 80 $^{\circ}\text{C}$ in nitrogen atmosphere. The pristine N-GQDs and PEDOT-PSS gas sensors were also fabricated and tested for comparison. The fabricated N-GQDs/PEDOT-PSS nanocomposite gas sensor is displayed in Fig. 1e-f.

Characterization methods

Transmission electron microscopy (TEM) was examined under LEO 912AB electron microscopy operated at an accelerating voltage of 120 kV. Field emission scanning electron microscopy (FESEM) was measured with S-4160 electron microscopy. X-ray diffraction (XRD) pattern was performed using a powder XRD system (Philips1825) with Cu K α irradiation ($\lambda = 1.54 \text{ \AA}$), operating at 40 kV and with a cathode current 20 mA. X-ray photoemission spectroscopy (XPS) measurements were performed on a ThermoVG scientific (VG multilab 2000) with Al K α radiation. The UV-vis absorption spectrum and the photoluminescence (PL) spectrum of N-GQDs in water were recorded using a 5300pc spectrophotometer and a fluorimeter, SPEX flouolog-3, with slit width of 0.5 mm. Atomic force microscopic (AFM) image was performed in the tapping mode with a Dualscope/Rasterscope C26 DME (Mahar Fan Abzar Co, Iran). Raman spectrum was taken using a Nanofinder 30 (Tokyo Instruments Co., Osaka, Japan). The sensor resistances were measured in a closed steel chamber (lab-made) with a LCR meter (Pintek-LCR900) and vapor gas flows were injected into the closed steel chamber by a mass flow meter (Alicat scientific, Tucson, USA). The reference humidity and sensor temperature were monitored by PT100 and HIH4000, respectively. The response and selectivity of the gas sensors were then assessed by the standard flow-through method towards methanol, ethanol,

acetone, toluene, water, chlorobenzene, and propanol with gas concentrations ranging from 1 ppm to 1000 ppm at room temperature. A constant flux of synthetic air of about $50 \text{ cm}^3 \text{ min}^{-1}$ was mixed with the target gas source at different flow rate ratios to desired concentrations using mass flow controllers. All experiments were performed at room temperature ($25 \pm 2 \text{ }^\circ\text{C}$) and the relative humidity of $10 \pm 2 \%$. The sensitivity defined by the following equation:

$$\text{Sensitivity} = \frac{\Delta R}{R_0} \times 100 \quad (1)$$

and

$$\Delta R = R_{gas} - R_0 \quad (2)$$

where R_0 and R_{gas} are the resistances of the sensor in synthetic air and target gas, respectively.

Results and discussion

Figure 2a show the typical TEM image of as-prepared N-GQDs. It is found that N-GQDs are relatively uniform with the diameters of 2-7 nm, which similar to those of N-GQDs prepared electrochemically [27]. The corresponding AFM image exhibited its height distribution of 1–2.5 nm which recommend that most of the N-GQDs comprise of 1–5 graphene layers (Fig. 2b-c).

The UV-vis absorption spectrum of N-GQDs shows the absorption band at 270 nm (Fig. 3a), which is blue shifted by 50 nm with respected to that of hydrothermally synthesized GQDs [28]. It has been reported that isolated sp^2 clusters with a size of 3 nm within the carbon-oxygen sp^3 matrix could yield band gaps consistent with blue emission due to the localization of electron-hole pairs, suggesting the size and surface effects bring about an significant contribution to the observed blue shift for N-GQDs [29,30,27]. Note that the previous observations proved the

strong electron-withdrawing ability of the N atoms within the conjugated C plane could contribute to PL blue shift [30,31,27]. The PL spectrum of N-GQDs shows a PL emission peak centered at 500 nm (Fig. 3b), when the excitation wavelength was fixed at 300 nm. Moreover, it is worth mentioning that the resultant N-GQDs are very stable in aqueous solution without aggregation or fluorescence degradation after storage for several month at room temperature. Figure 3c shows the Raman spectra of N-GQDs which exhibits two characteristic peaks centered at 1324 and 1587 cm^{-1} , corresponding to the D and G bands of carbon materials, respectively. It was observed that the I_D/I_G ratio of N-GQDs is 0.61. The low ratio of D to G bands not only indicates their electronic conjugate statues but also presents the production of relatively high quality N-GQDs by hydrothermal process of citric acid [32,27].

Figure 3d shows typical XRD pattern for the N-GQDs which showed a broader diffraction peak at 25° , with respect to graphene film [27]. The corresponding d-spacing of N-GQDs is approximately 0.34 nm, according to Bragg's law: $2d\sin\theta = n\lambda$, where n is an integer determined by the given order, and λ is the wavelength. It is worth pointing out that the as-prepared N-GQDs did not show any diffractions in the $2\theta \approx 10^\circ$ region characteristic of graphene oxides, evidently suggesting that the N-GQDs are different from graphene oxide [27,33,23]. XPS measurement was carried out to determine the composition of the as-prepared N-GQDs. The XPS spectra of the N-GQDs show a predominant graphitic C 1s peak at about 284 eV and an O 1s peak at about 532 eV (Fig. 4). The O to C atomic ratio for N-GQDs is almost 0.663, demonstrating that the N-GQDs have a high oxidation level. The N to C atomic ratio was calculated to be 0.058, which is remarkably higher than that of the N-GQDs prepared electrochemically (0.043) [27,30]. A pronounced N 1s spectrum of the N-GQDs shows the presence of both pyridine-like (398.3 eV) and pyrrolic-like (399.6 eV) N atoms [27,34]. This confirmed the successful incorporation of N

atoms into the N-GQDs by hydrothermal process in the presence of urea. The SEM images of drop-coated pure PEDOT-PSS and N-GQDs/PEDOT-PSS composite films showed that the N-GQDs were homogeneously dispersed into the PEDOT-PSS matrix without obvious agglomeration (Fig. 5). This was ascribed to the O-rich groups on the N-GQDs surface which ensured the strong bonding with PEDOT-PSS [35,27].

Figure 6a-b show the dynamic responses of the pristine PEDOT-PSS and N-GQDs/PEDOT-PSS nanocomposite gas sensors towards various concentration of methanol, ethanol, and acetone at room temperature, respectively. It indicates that the sensors exhibit good repeatability of response towards various concentration of VOCs. The sensitivity of both sensors increase upon exposure to VOCs and recover to the initial value upon the removal of VOCs in air. In addition, the both sensors showed the higher sensitivity to methanol as compared to other VOCs. Furthermore, the sensitivity of N-GQDs/PEDOT-PSS nanocomposite gas sensor is increased by more than a factor of about twelve as compared to pristine PEDOT-PSS gas sensor at 50 ppm of methanol (time = 200 s). The resistance changing behaviors may be attributed to the adsorption and desorption of VOC molecules of the sensing films. The details of sensing mechanism for N-GQDs/PEDOT-PSS nanocomposite gas sensor will be discussed in further. In addition, it can be observed that N-GQDs/PEDOT-PSS nanocomposite gas sensor has much lower initial resistance than pristine PEDOT-PSS. The conductivities of pristine PEDOT-PSS and N-GQDs/PEDOT-PSS nanocomposite sensing films measured by 4-point probe technique at 10 nA applied current are 650 and 1365 $\text{S}\cdot\text{cm}^{-1}$, respectively. It corresponds to a significant increase of charge carrier concentration due to N-GQDs incorporation. From the results, the conductivity of PEDOT-PSS is increased by more than a factor of 2 after the N-GQDs addition. Thus, N-GQDs may form

conduction channels that substantially enhance the charge transport process through the PEDOT-PSS matrix.

The PEDOT-PSS based gas sensors usually operate at rather low temperatures with respect to gas sensors based on metal oxide [26,11,36]. It can be seen that the N-GQDs/PEDOT-PSS nanocomposite gas sensor shows low sensitivity to methanol with increase of temperature (Fig. 7). Therefore, the optimal temperature of the N-GQDs/PEDOT-PSS nanocomposite gas sensor for VOCs detection was found to be room temperature. Since the interaction between N-GQDs/PEDOT-PSS nanocomposite film and VOCs gas is exothermic, the activation energy of desorption is larger than that of the adsorption methanol molecules of nanocomposite sensing film. This revealed that the decrease in sensitivity at higher temperatures is resulted from the higher desorption rate of methanol gas.

The response time, defined as the time to reach 90 % of the maximum total resistance change of the pristine PEDOT-PSS and N-GQDs/PEDOT-PSS nanocomposite gas sensors towards methanol are estimated to be 164 s and 12 s, respectively (Fig. 8). Moreover, the resistance of N-GQDs/PEDOT-PSS nanocomposite gas sensor could recover almost completely to the initial value within the pure air exposure times of 40 s while the PEDOT-PSS gas sensor shows undesirable resistance drift. Thus, N-GQDs/PEDOT-PSS nanocomposite gas sensor exhibits relatively short response and recovery times compared with pristine PEDOT-PSS one. The slower response and recovery of pristine PEDOT-PSS gas sensor may be due to low diffusion and short penetration depth of gas molecules on very smooth surface of the PEDOT-PSS sensing film [26,11].

In order to investigate the selectivity of pristine PEDOT-PSS and N-GQDs/PEDOT-PSS nanocomposite gas sensors, they were exposed to a variety of VOCs including methanol,

ethanol, acetone, toluene, chlorobenzene, propideanol, and water with the concentration of 100 ppm at room temperature. Fig. 9 demonstrates the gas response of pristine PEDOT-PSS and N-GQDs/PEDOT-PSS nanocomposite gas sensors to various VOCs. It can be seen that the N-GQDs/PEDOT-PSS nanocomposite gas sensor shows high response to methanol while is almost sensitive to the other VOCs. At 100 ppm of methanol, the sensitivity of N-GQDs/PEDOT-PSS nanocomposite gas sensor increases further to 154.4 % which is almost 12 times as high as that of pristine PEDOT-PSS gas sensor. Therefore, the sensitivity of pure N-GQDs, pristine PEDOT-PSS and N-GQDs/PEDOT-PSS nanocomposite gas sensors to methanol was depicted at concentration ranging from 1 ppm to 1000 ppm at room temperature in Fig. 10a. At 1000 ppm concentration, the sensitivity of pure N-GQDs, pristine PEDOT-PSS and N-GQDs/PEDOT-PSS nanocomposite gas sensors are 10 %, 35 %, and 180 %, respectively. With N-GQDs addition, the sensitivity and selectivity to methanol are substantially improved. It is seen that the room temperature response of pure N-GQDs to methanol is much lower than that of pristine PEDOT-PSS, but the gas response is significantly enhanced after preparation of N-GQDs/PEDOT-PSS nanocomposite film. Thus, N-GQDs enhances methanol interaction leading the higher charge reduction only when it is included in PEDOT-PSS network. At low concentration (1–50 ppm), pristine PEDOT-PSS is still able to respond to methanol with gas response ranging from 0.5–10 %. However, the gas response of N-GQDs/PEDOT-PSS nanocomposite gas sensor to methanol is still higher than that of undoped one with the gas response ranging from 13.5 % to 134 % (Fig. 7b). Moreover, the gas response of pristine N-GQDs, and PEDOT-PSS gas sensors to methanol are not significant different in the low concentration range (1–50 ppm). The detection limit of methanol for N-GQDs/PEDOT-PSS nanocomposite gas sensor is 5 ppm at the room temperature.

It is worth mentioning that the dynamic range of methanol for fabricated nanocomposite gas sensor is then estimated to be 10-200 ppm.

Sensing mechanism of N-GQDs/PEDOT-PSS nanocomposite gas sensor

Organic analytes and VOCs are not reactive at room temperature, so it is hard to detect VOCs with their chemical reactions with conducting polymers. Therefore, typical sensing mechanisms including absorbing and swelling of polymers have been proposed for the detection of VOCs by conducting polymer systems [36,37]. In this case, the resistance changing behavior of N-GQDs/PEDOT-PSS nanocomposite gas sensor may be explained based on two possible mechanisms: i) When methanol molecules are adsorbed on the surface of N-GQDs/PEDOT-PSS nanocomposite by physisorption, hence the holes of conductive N-GQDs/PEDOT-PSS nanocomposite surface will interact with the electron-donating methanol analyte. This leads to not only increase of delocalization degree of conjugated π -electrons of sensing film but also decrease in charge carriers resulting in the decline of the electrical conductivity of the sensing film [38,35,11]. This mechanism is widely adopted for explanation of the change in conductivity of conductive polymer to acidic/basic analytes (doping/dedoping process). ii) In addition to adsorption, swelling process from the diffusion of analyte into the conducting polymer systems is widely observed phenomenon in the VOCs detection. When methanol molecules diffuse into polymer matrix, electron hopping process becomes more difficult because the PEDOT interchain distance increases due to the swelling process [39,37,36]. In the case of N-GQDs/PEDOT-PSS nanocomposite gas sensor, N-GQDs embedded into polymer matrix acts as conductive pathways that favor the hopping of electrons. The swelling process can cause the N-GQDs to stay apart, disrupting conductive pathways in the sensing film. The increase of PEDOT distance and decrease of N-GQD's conductive pathways occur simultaneously, leading to significant increase

in resistance of the N-GQDs/PEDOT-PSS nanocomposite gas sensor upon methanol exposure and therefore enhanced methanol response. Based on the results, direct charge transfer process appears to be the most probable dominant process for methanol-sensing of the N-GQDs/PEDOT-PSS nanocomposite gas sensor due to the observed high response and selectively to polar molecules.

Conclusion

The pure N-GQDs, pristine PEDOT-PSS and N-GQDs/PEDOT-PSS nanocomposite gas sensors has been successfully fabricated and characterized for VOC vapors sensing. The N-GQDs was synthesized by simple hydrothermal process of citric acid with a diameter of 2-7 nm and N to C atomic ratio of 0.058. This N-GQDs/PEDOT-PSS nanocomposite gas sensor exhibit high sensing performance to methanol with concentration ranging from 1 ppm to 1000 ppm at room temperature. The N-GQDs/PEDOT-PSS nanocomposite gas sensor enhance methanol sensing properties by 12 times compared to pristine PEDOT-PSS at room temperature. Direct charge transfers and swelling process are among possible sensing mechanisms of the N-GQDs/PEDOT-PSS nanocomposite gas sensor. From the results, the proposed nanocomposite gas sensor offers several distinct advantages over some other sensors including high sensing performances, fast response and recovery times, low temperature processing, high productivity and simplicity. Moreover, it will be useful for development of future wearable electronic technology.

References

1. Casalnuovo IA, Di Pierro D, Coletta M, Di Francesco P (2006) Application of electronic noses for disease diagnosis and food spoilage detection. *Sensors* 6 (11):1428-1439
2. Peris M, Escuder-Gilabert L (2009) A 21st century technique for food control: Electronic noses. *Analytica Chimica Acta* 638 (1):1-15
3. Tung TT, Castro M, Kim TY, Suh KS, Feller J-F (2012) Graphene quantum resistive sensing skin for the detection of alteration biomarkers. *Journal of Materials Chemistry* 22 (40):21754-21766

4. Srivastava P, Pandit G, Sharma S, Rao AM (2000) Volatile organic compounds in indoor environments in Mumbai, India. *Science of the Total Environment* 255 (1):161-168
5. Wang L, Chen W, Xu D, Shim BS, Zhu Y, Sun F, Liu L, Peng C, Jin Z, Xu C (2009) Simple, Rapid, Sensitive, and Versatile SWNT– Paper Sensor for Environmental Toxin Detection Competitive with ELISA. *Nano letters* 9 (12):4147-4152
6. Arasaradnam RP, Quraishi N, Kyrou I, Nwokolo CU, Joseph M, Kumar S, Bardhan KD, Covington JA (2011) Insights into 'fermentonomics': evaluation of volatile organic compounds (VOCs) in human disease using an electronic 'e-nose'. *Journal of medical engineering & technology* 35 (2):87-91
7. Cheng Z, Li Q, Li Z, Zhou Q, Fang Y (2010) Suspended graphene sensors with improved signal and reduced noise. *Nano letters* 10 (5):1864-1868
8. Robinson JT, Perkins FK, Snow ES, Wei Z, Sheehan PE (2008) Reduced graphene oxide molecular sensors. *Nano letters* 8 (10):3137-3140
9. Kong J, Franklin NR, Zhou C, Chapline MG, Peng S, Cho K, Dai H (2000) Nanotube molecular wires as chemical sensors. *science* 287 (5453):622-625
10. Tung TT, Kim TY, Shim JP, Yang WS, Kim H, Suh KS (2011) Poly (ionic liquid)-stabilized graphene sheets and their hybrid with poly (3, 4-ethylenedioxythiophene). *Organic Electronics* 12 (12):2215-2224
11. Seekaew Y, Lokavee S, Phokharatkul D, Wisitsoraat A, Kerdcharoen T, Wongchoosuk C (2014) Low-cost and flexible printed graphene–PEDOT: PSS gas sensor for ammonia detection. *Organic Electronics* 15 (11):2971-2981
12. Wu X, Li F, Wu W, Guo T (2014) Flexible organic light emitting diodes based on double-layered graphene/PEDOT: PSS conductive film formed by spray-coating. *Vacuum* 101:53-56
13. Huang X, Hu N, Gao R, Yu Y, Wang Y, Yang Z, Kong ES-W, Wei H, Zhang Y (2012) Reduced graphene oxide–polyaniline hybrid: preparation, characterization and its applications for ammonia gas sensing. *Journal of Materials Chemistry* 22 (42):22488-22495
14. Ponomarenko L, Schedin F, Katsnelson M, Yang R, Hill E, Novoselov K, Geim A (2008) Chaotic Dirac billiard in graphene quantum dots. *Science* 320 (5874):356-358
15. MingáLi C (2012) One-step and high yield simultaneous preparation of single-and multi-layer graphene quantum dots from CX-72 carbon black. *Journal of Materials Chemistry* 22 (18):8764-8766
16. Shen J, Zhu Y, Yang X, Li C (2012) Graphene quantum dots: emergent nanolights for bioimaging, sensors, catalysis and photovoltaic devices. *Chemical Communications* 48 (31):3686-3699
17. Lu J, Yeo PSE, Gan CK, Wu P, Loh KP (2011) Transforming C60 molecules into graphene quantum dots. *Nature nanotechnology* 6 (4):247-252
18. Liu R, Wu D, Feng X, Müllen K (2011) Bottom-up fabrication of photoluminescent graphene quantum dots with uniform morphology. *Journal of the American Chemical Society* 133 (39):15221-15223
19. Mahyari M, Shaabani A, Bide Y (2013) Gold nanoparticles supported on supramolecular ionic liquid grafted graphene: a bifunctional catalyst for the selective aerobic oxidation of alcohols. *RSC Advances* 3 (44):22509-22517
20. Mahyari M, Shaabani A (2014) Nickel nanoparticles immobilized on three-dimensional nitrogen-doped graphene as a superb catalyst for the generation of hydrogen from the hydrolysis of ammonia borane. *Journal of Materials Chemistry A* 2 (39):16652-16659

21. SadeghíLaeini M (2014) Aqueous aerobic oxidation of alkyl arenes and alcohols catalyzed by copper (II) phthalocyanine supported on three-dimensional nitrogen-doped graphene at room temperature. *Chemical Communications* 50 (58):7855-7857
22. GavGANi JN, Adelnia H, Gudarzi MM (2014) Intumescent flame retardant polyurethane/reduced graphene oxide composites with improved mechanical, thermal, and barrier properties. *Journal of Materials Science* 49 (1):243-254
23. Dehsari HS, Shalamzari EK, GavGANi JN, Taromi FA, Ghanbary S (2014) Efficient preparation of ultralarge graphene oxide using a PEDOT: PSS/GO composite layer as hole transport layer in polymer-based optoelectronic devices. *RSC Advances* 4 (98):55067-55076
24. Hosseini H, Behbahani M, Mahyari M, Kazerooni H, Bagheri A, Shaabani A (2014) Ordered carbohydrate-derived porous carbons immobilized gold nanoparticles as a new electrode material for electrocatalytical oxidation and determination of nicotinamide adenine dinucleotide. *Biosensors and Bioelectronics* 59:412-417
25. Hosseini H, Mahyari M, Bagheri A, Shaabani A (2014) A novel bioelectrochemical sensing platform based on covalently attachment of cobalt phthalocyanine to graphene oxide. *Biosensors and Bioelectronics* 52:136-142
26. Hasani A, Dehsari HS, GavGANi JN, Shalamzari EK, Salehi A, Taromi FA, Mahyari M (2015) Sensor for volatile organic compounds using an interdigitated gold electrode modified with a nanocomposite made from poly (3, 4-ethylenedioxythiophene)-poly (styrenesulfonate) and ultra-large graphene oxide. *Microchimica Acta* 182 (7-8):1551-1559
27. Li Y, Zhao Y, Cheng H, Hu Y, Shi G, Dai L, Qu L (2011) Nitrogen-doped graphene quantum dots with oxygen-rich functional groups. *Journal of the American Chemical Society* 134 (1):15-18
28. Pan D, Zhang J, Li Z, Wu M (2010) Hydrothermal route for cutting graphene sheets into blue-luminescent graphene quantum dots. *Advanced Materials* 22 (6):734-738
29. Eda G, Lin Y-Y, Mattevi C, Yamaguchi H, Chen H-A, Chen I-S, Chen C-W, Chhowalla M (2010) Blue photoluminescence from chemically derived graphene oxide. *Advanced Materials* 22 (4):505
30. Li M, Wu W, Ren W, Cheng H-M, Tang N, Zhong W, Du Y (2012) Synthesis and upconversion luminescence of N-doped graphene quantum dots. *Applied Physics Letters* 101 (10):103107
31. Gong K, Du F, Xia Z, Durstock M, Dai L (2009) Nitrogen-doped carbon nanotube arrays with high electrocatalytic activity for oxygen reduction. *science* 323 (5915):760-764
32. Reich S, Thomsen C (2004) Raman spectroscopy of graphite. *Philosophical Transactions of the Royal Society of London A: Mathematical, Physical and Engineering Sciences* 362 (1824):2271-2288
33. Jeong HY, Kim JY, Kim JW, Hwang JO, Kim J-E, Lee JY, Yoon TH, Cho BJ, Kim SO, Ruoff RS (2010) Graphene oxide thin films for flexible nonvolatile memory applications. *Nano letters* 10 (11):4381-4386
34. Qu L, Liu Y, Baek J-B, Dai L (2010) Nitrogen-doped graphene as efficient metal-free electrocatalyst for oxygen reduction in fuel cells. *ACS nano* 4 (3):1321-1326
35. Jian J, Guo X, Lin L, Cai Q, Cheng J, Li J (2013) Gas-sensing characteristics of dielectrophoretically assembled composite film of oxygen plasma-treated SWCNTs and PEDOT/PSS polymer. *Sensors and Actuators B: Chemical* 178:279-288
36. Lin C-Y, Chen J-G, Hu C-W, Tunney JJ, Ho K-C (2009) Using a PEDOT: PSS modified electrode for detecting nitric oxide gas. *Sensors and Actuators B: Chemical* 140 (2):402-406

37. Bai H, Shi G (2007) Gas sensors based on conducting polymers. *Sensors* 7 (3):267-307
38. Kwon OS, Park E, Kweon OY, Park SJ, Jang J (2010) Novel flexible chemical gas sensor based on poly (3, 4-ethylenedioxythiophene) nanotube membrane. *Talanta* 82 (4):1338-1343
39. Crispin X, Marciniak S, Osikowicz W, Zotti G, van der Gon A, Louwet F, Fahlman M, Groenendaal L, De Schryver F, Salaneck WR (2003) Conductivity, morphology, interfacial chemistry, and stability of poly (3, 4-ethylene dioxythiophene)-poly (styrene sulfonate): A photoelectron spectroscopy study. *Journal of polymer science Part B: Polymer physics* 41 (21):2561-2583

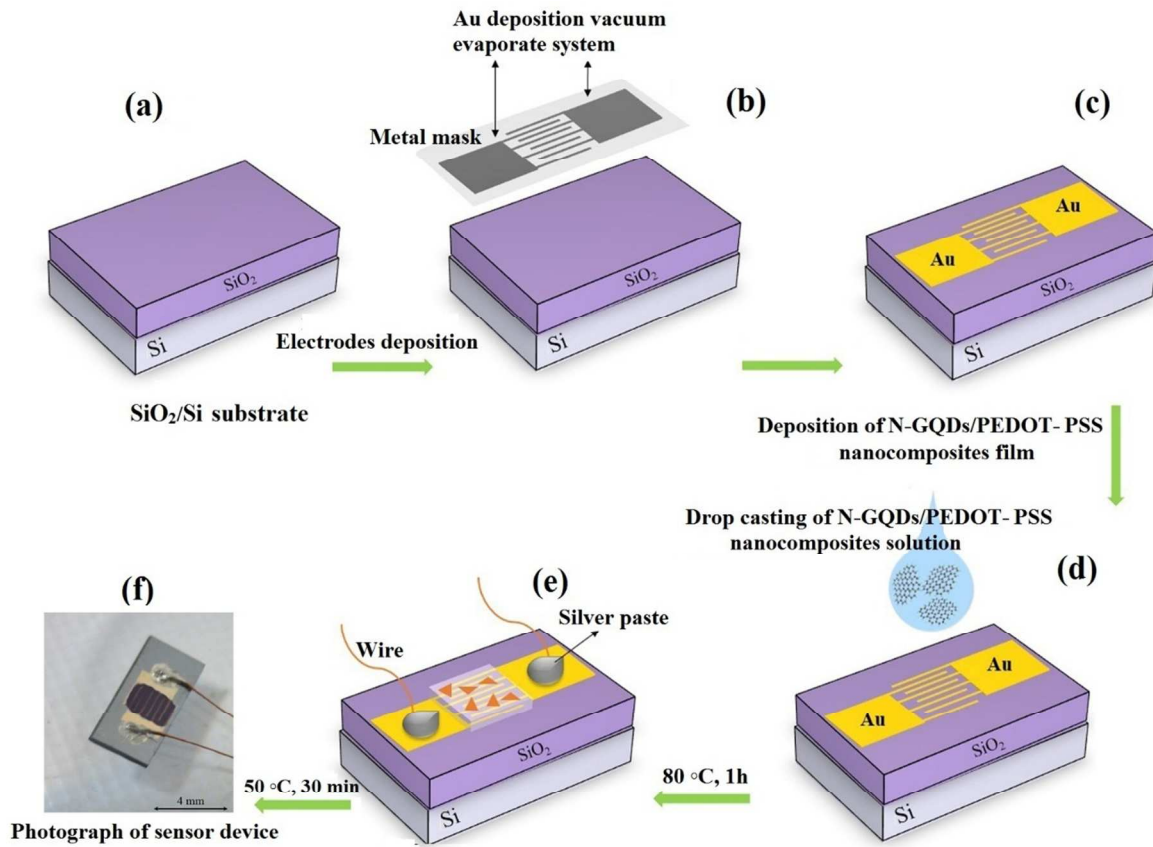


Fig. 1 Schematic steps of gas sensor fabrication process.

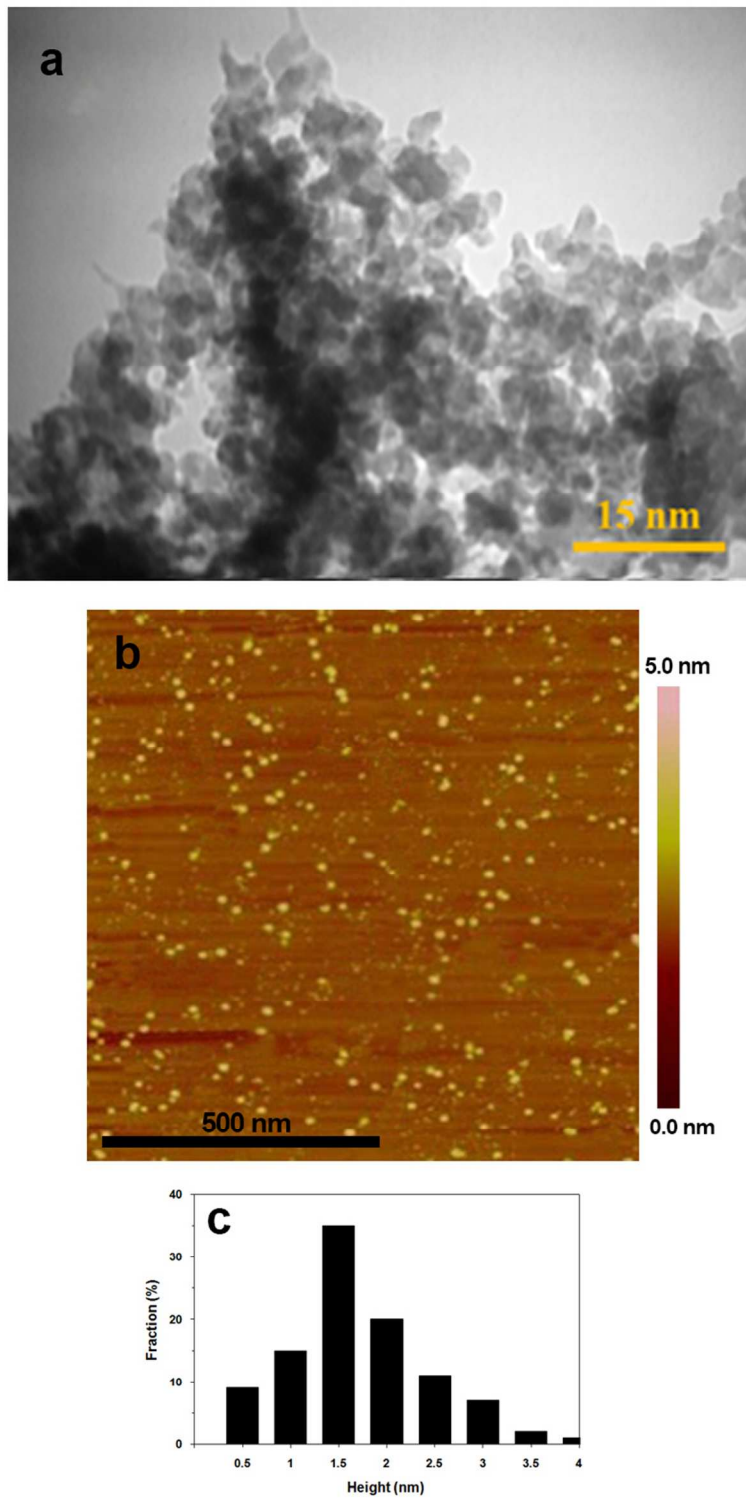


Fig. 2 (a) TEM image of as-prepared N-GQDs, (b) AFM image of N-GQDs on Si substrate, and (c) Height distribution of N-GQDs.

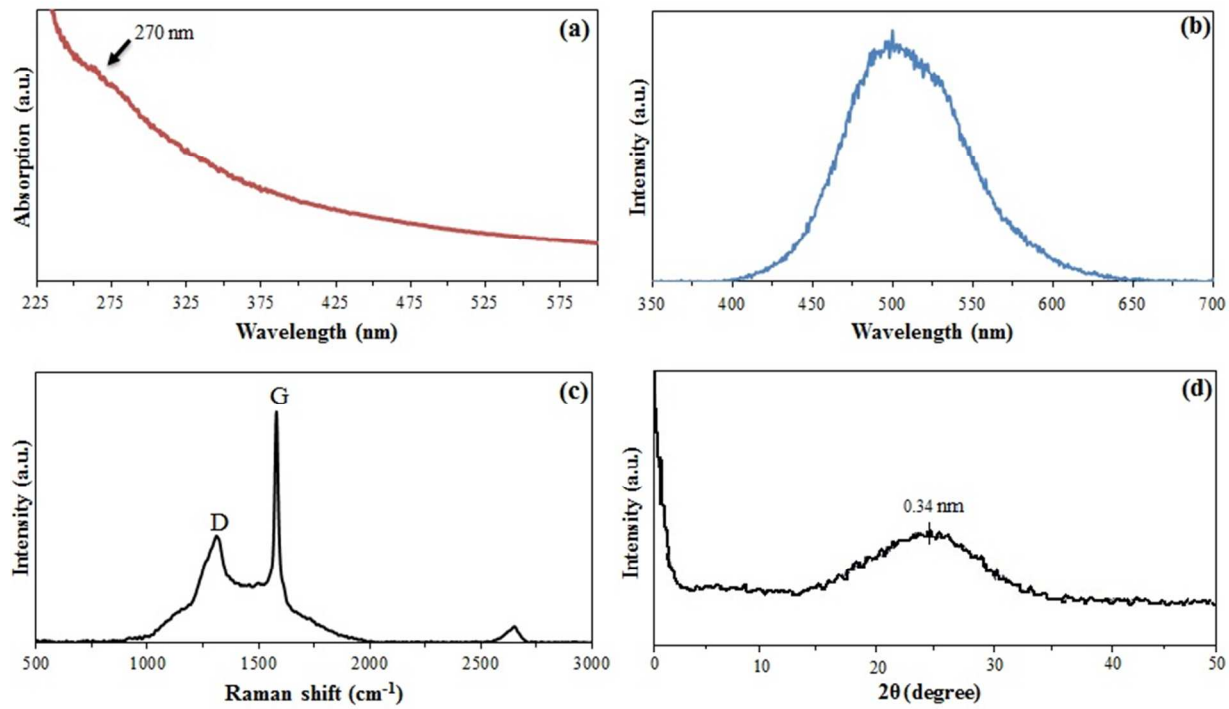


Fig. 3 (a) UV-vis absorption spectrum, (b) PL spectrum, (c) Raman spectrum and (d) XRD pattern of as-prepared N-GQDs.

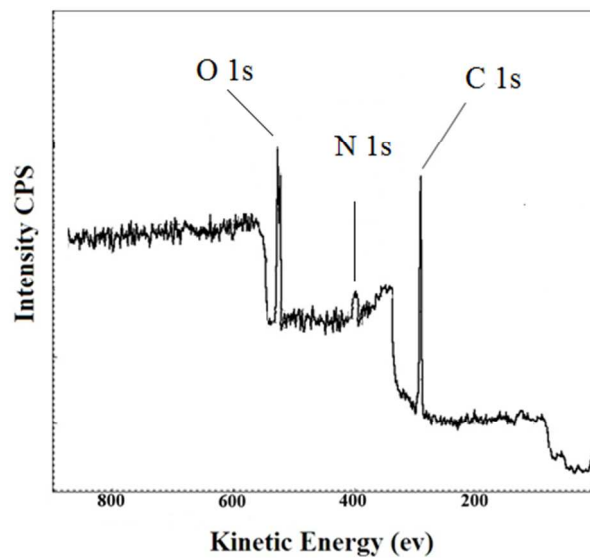


Fig. 4 Survey XPS spectrum of as-prepared N-GQDs.

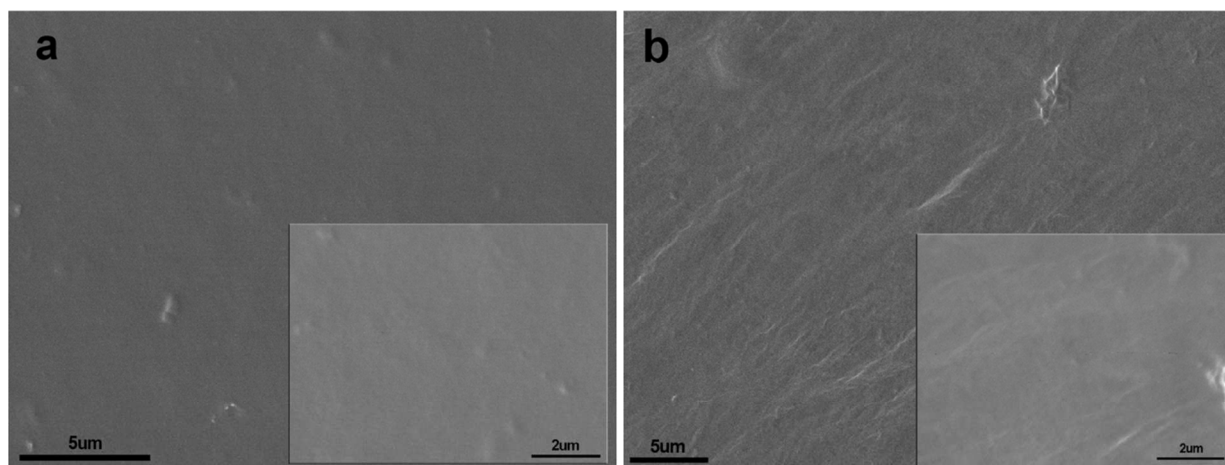


Fig. 5 SEM images of the pristine PEDOT-PSS (a), and N-GQDs/PEDOT-PSS nanocomposite films (b) in two different magnifications. The films were formed with drop coating.

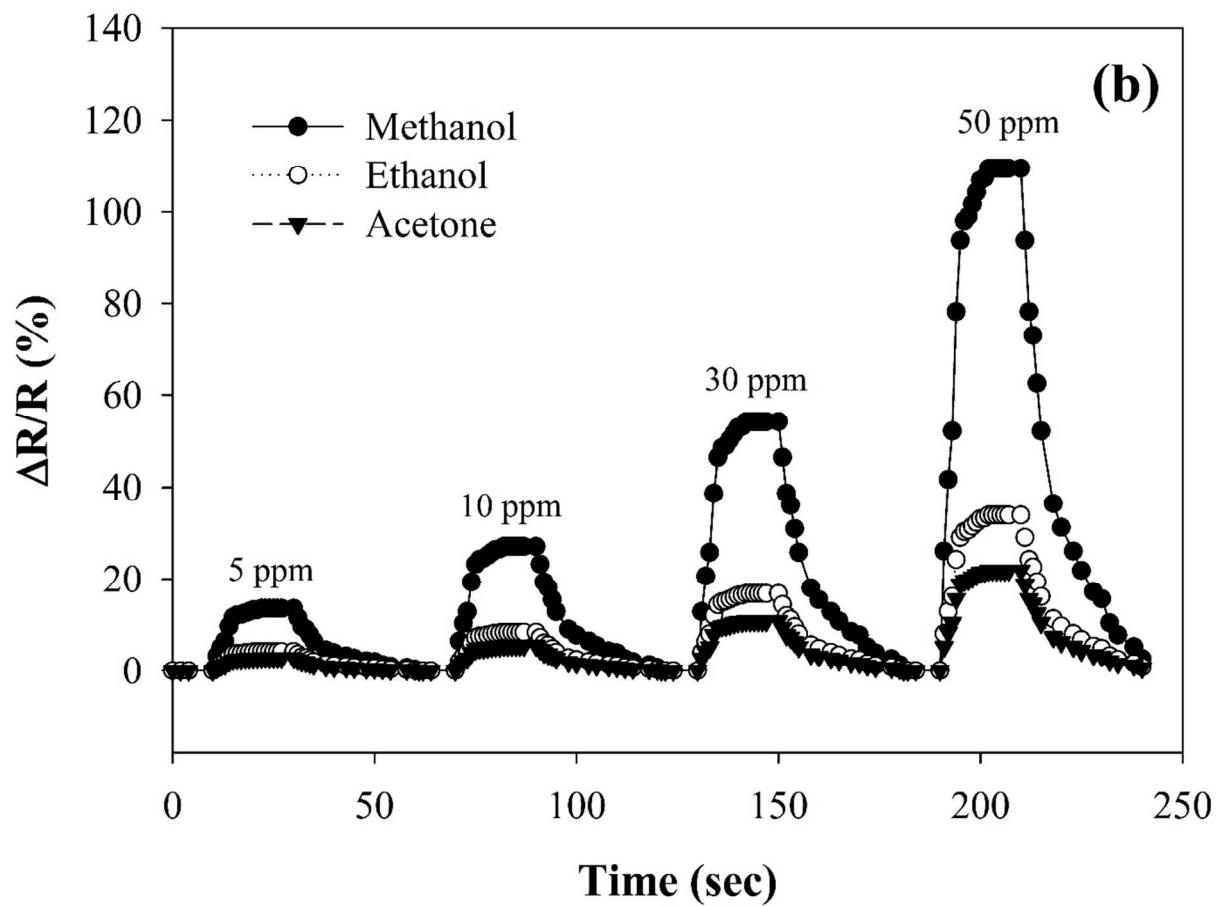


Fig. 6 Dynamic responses of (a) pristine PEDOT-PSS, and (b) N-GQDs/PEDOT-PSS nanocomposite gas sensors to various concentration of methanol, ethanol, and acetone at room temperature.

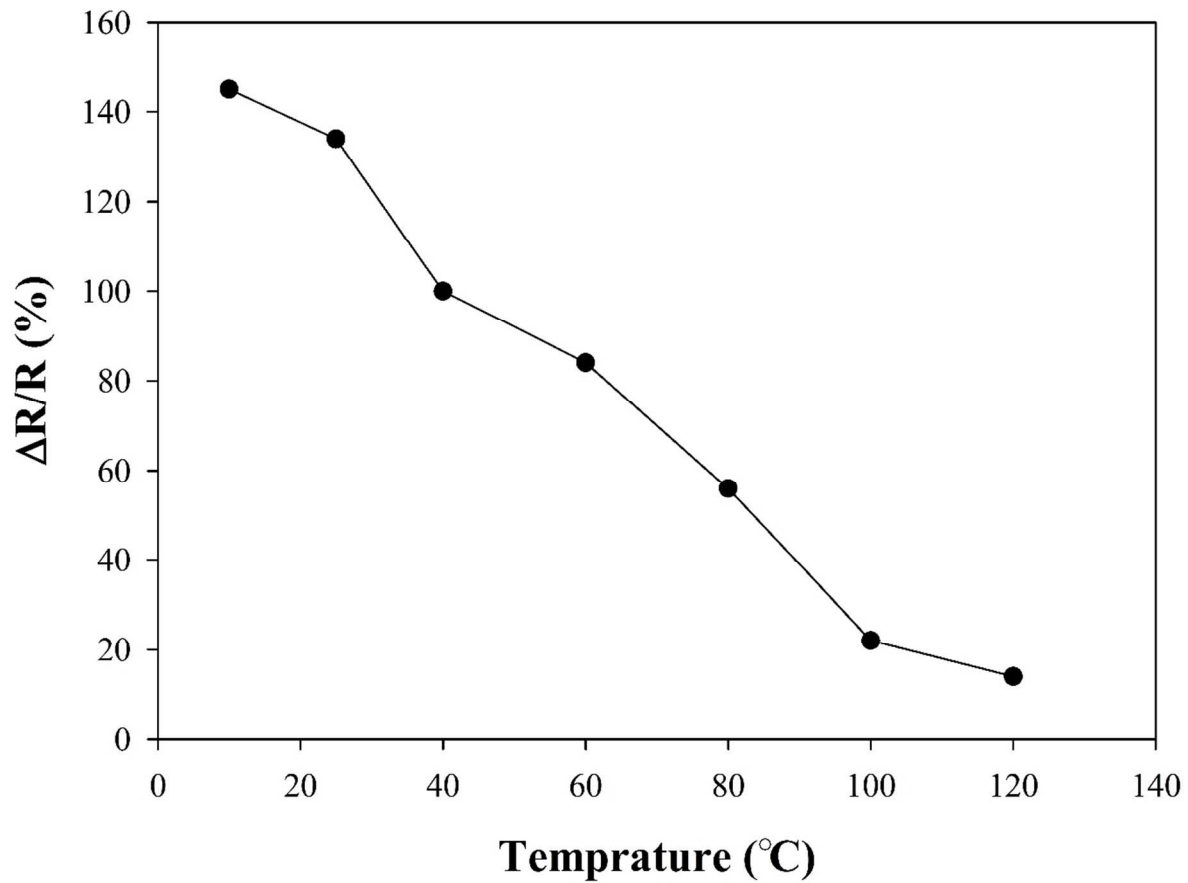
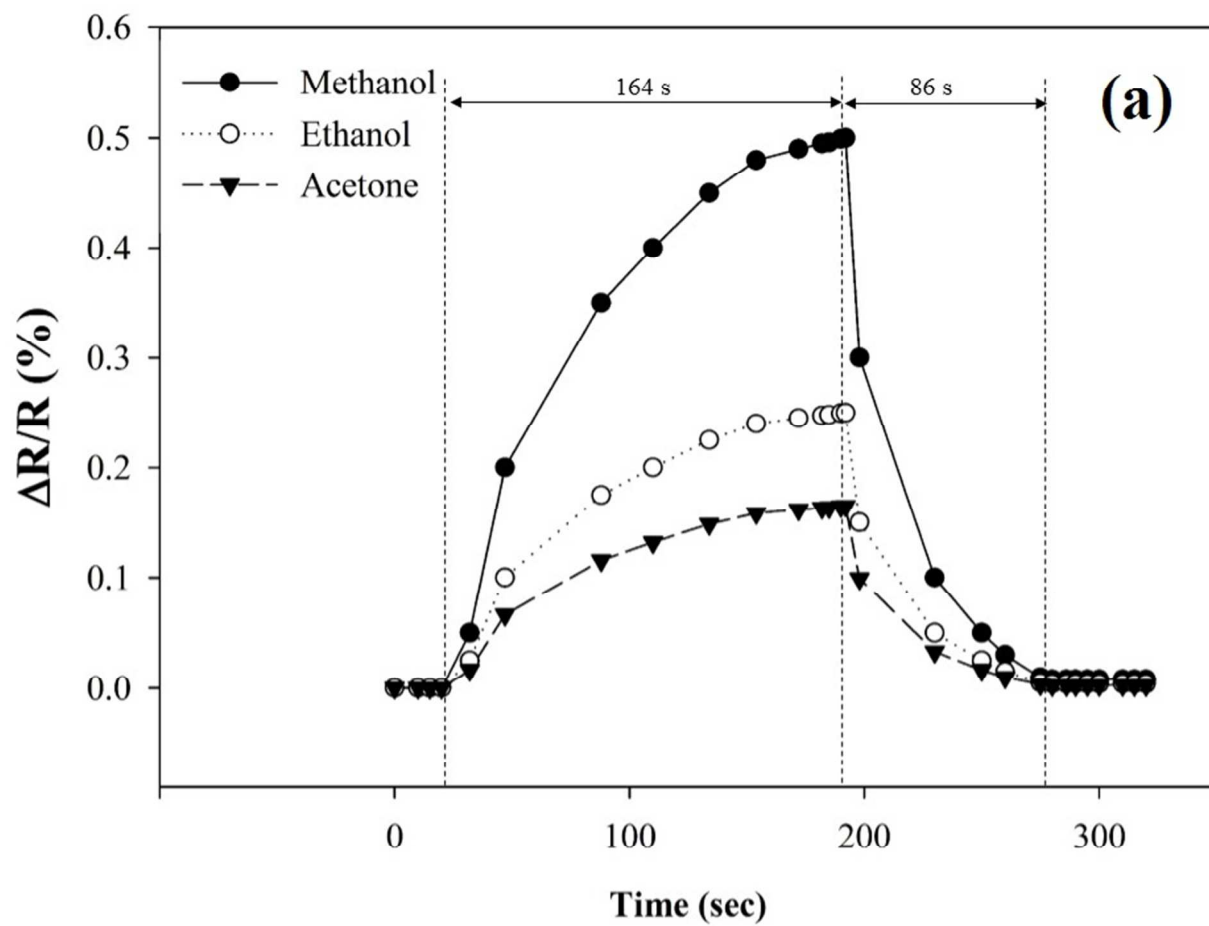


Fig. 7 Sensivity of the N-GQDs/PEDOT-PSS nanocomposite gas sensor as function of temperature towards 50 ppm methanol.



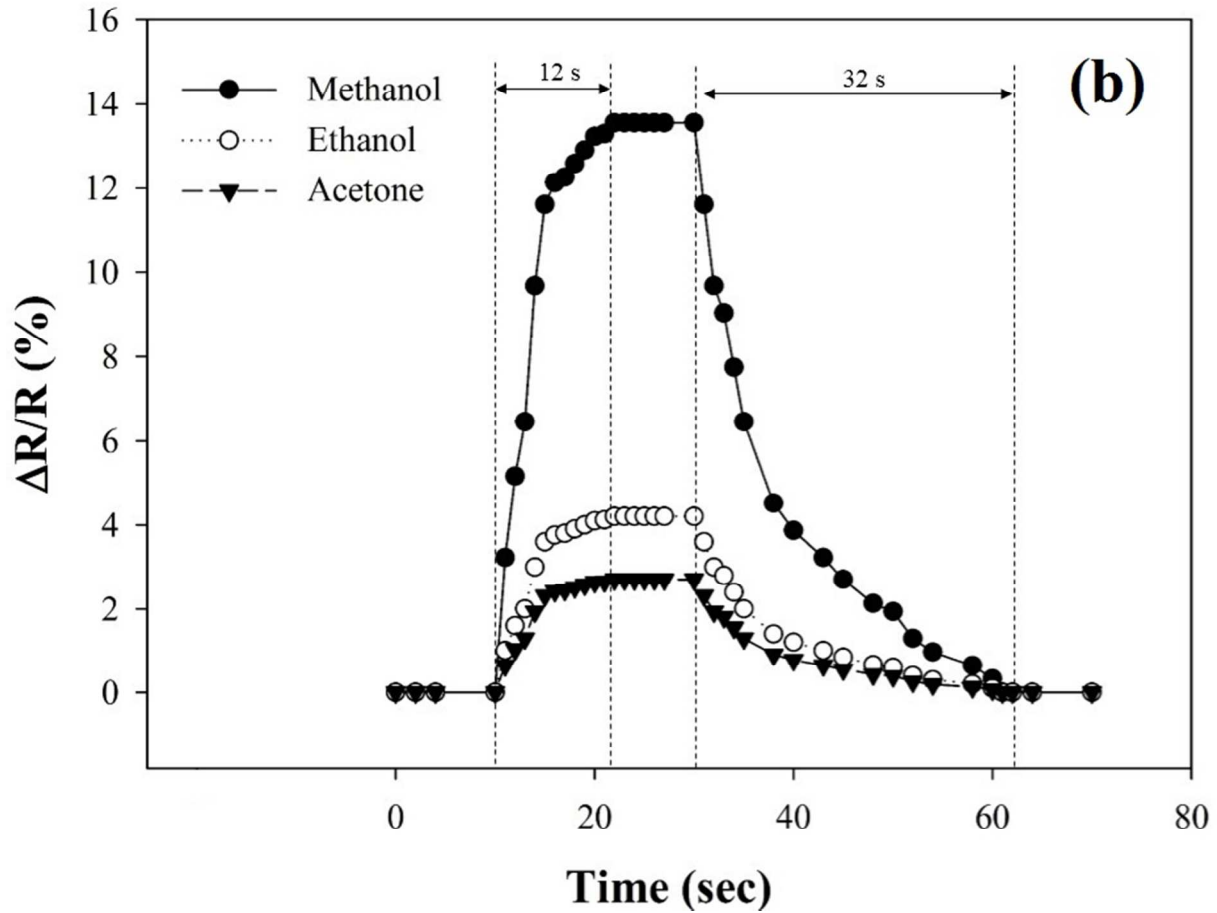


Fig. 8 Response and recovery times of the VOC gas sensors based on (a) pristine PEDOT-PSS and (b) N-GQDs/PEDOT-PSS nanocomposite for 100 ppm of methanol, ethanol, and acetone at room temperature

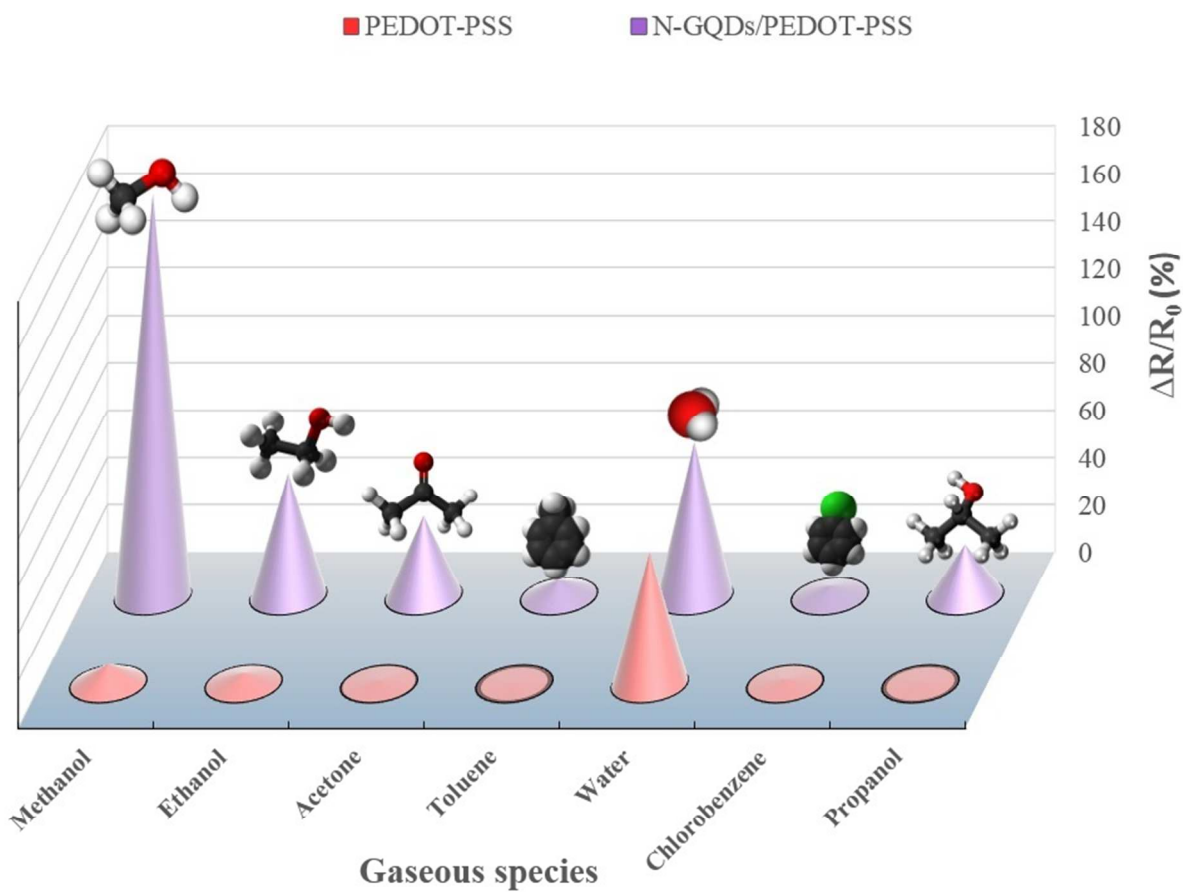
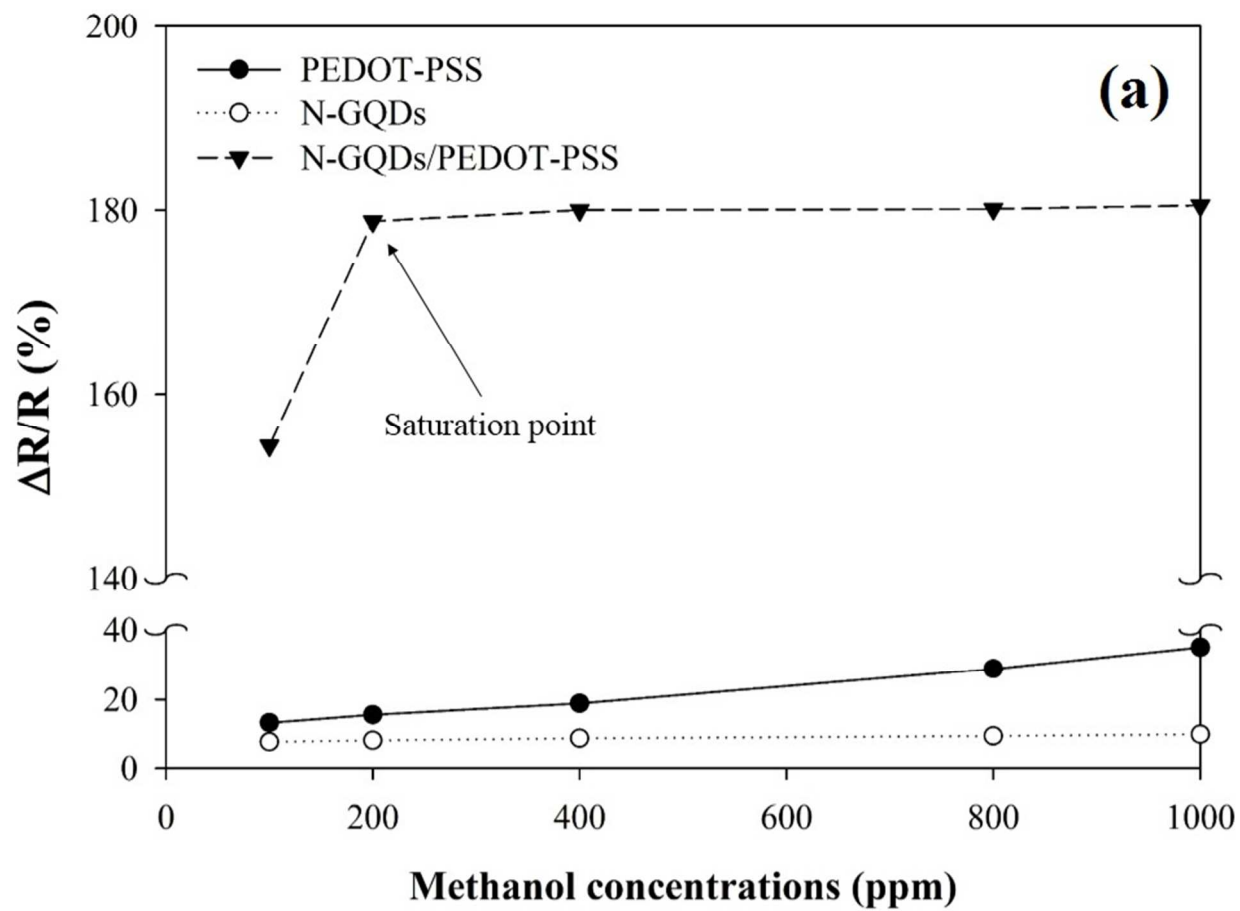


Fig. 9 Selectivity of the pristine PEDOT-PSS and N-GQDs/PEDOT-PSS nanocomposite gas sensors to various VOCs vapors of 100 ppm.



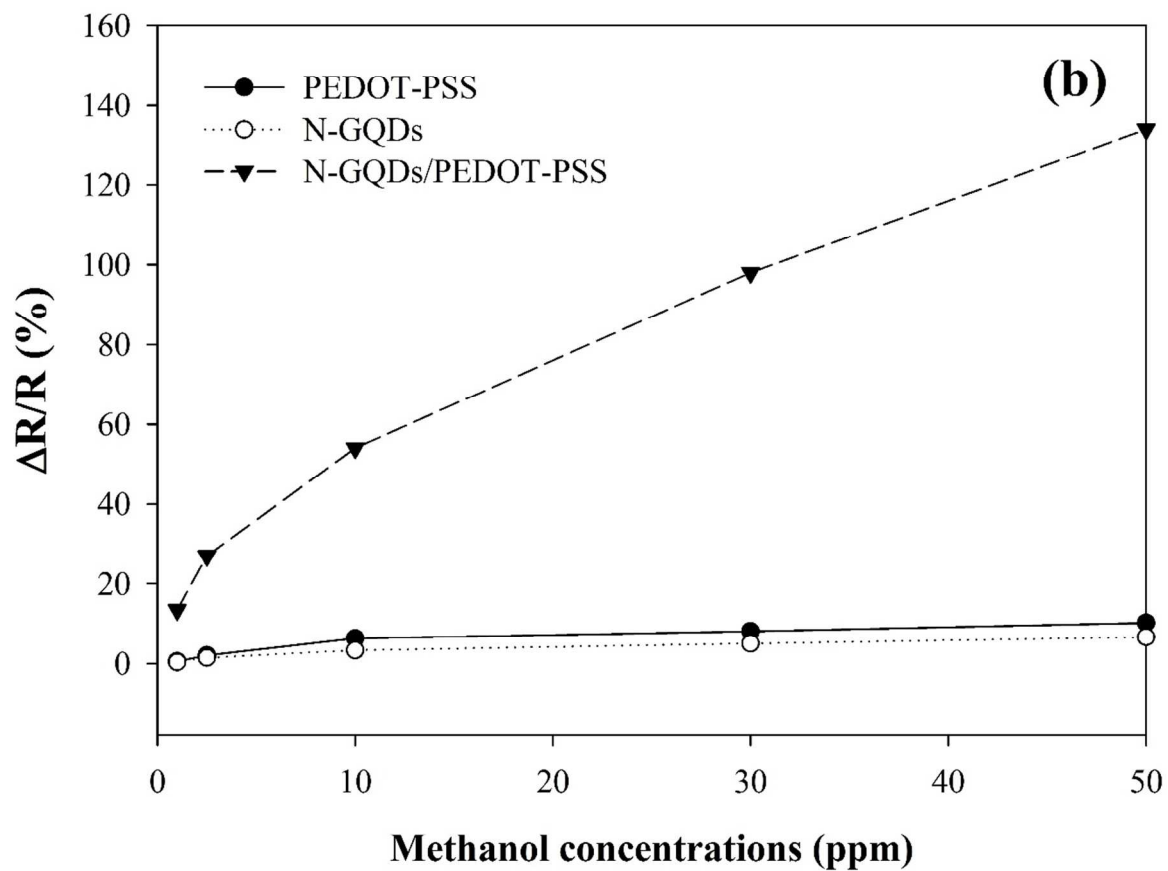
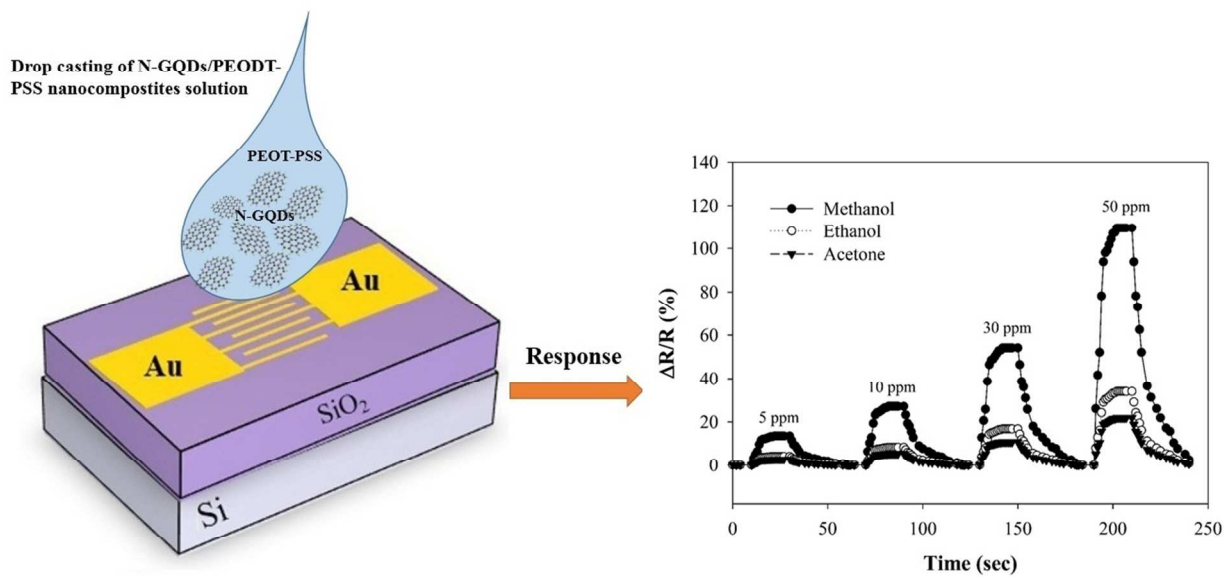


Fig. 10 Sensivity of pure N-GQDs, pristine PEDOT-PSS and N-GQDs/PEDOT-PSS nanocomposite gas sensors towards methanol, ethanol, and acetone at room temperature in the concentration range of (a) 1-1000 ppm, and (b) 1-50 ppm.



The highly efficient VOCs sensor based on N-doped graphene quantum dots (N-GQDs)/poly(3,4-ethylenedioxythiophene)-poly(styrenesulfonate)(PEDOT-PSS) was fabricated at room temperature.